In 8th International Symposium on Computational Fluid Dynamics,
Sept. 5-10, 1999, Bremen, Germany.

Computation of Mistuning Effects on Cascade Flutter

Mani Sadeghi* and Feng Liu†
Department of Mechanical and Aerospace Engineering
University of California, Irvine, CA 92697-3975

Abstract

This paper describes a computational method for predicting flutter of turbomachinery cascades with mistuned blades. The method solves the unsteady Euler/Navier-Stokes equations for multiple blade passages on a parallel computer using the Message Passing Interface (MPI). A second order implicit scheme with dual time-stepping and multigrid is used. In the parallel implementation, each blade passage is computed on one CPU with communication between neighboring passages performed by MPI. Each individual blade is capable of moving with its own independent frequency and also phase angle, therefore allowing flutter predictions for a cascade with mistuned blades. Both phase angle and frequency-mistuning are studied. It is found that frequency-mistuning has positive effect on preventing flutter for a turbine cascade.

1 Introduction

Turbomachinery designers are pushing for increased loading and reduced size and weight of compressor and turbine blade rows, particularly for aircraft engines. As such, the flutter of the turbomachinery blades may become a limiting factor in the design and performance of gas turbine engines. Accurate theoretical and computational methods in predicting the flutter boundary will enable us to achieve high performance and low cost by allowing adequate but not excessive design margins.

In a typical flutter calculation, the adjacent blades in a blade row are assumed to vibrate at the same frequency but with a constant phase difference, the Inter-Blade-Phase-Angle (IBPA). Single blade passages are usually used in order to minimize the computational effort. Consequently, a *phase-shifted* periodic boundary condition has to be applied when the IBPA is not zero. After the unsteady flow is determined, the Energy Method is used to determine if the system is stable or unstable for the particular frequency and phase shift. The use of the phase-shifted boundary condition and its implementation by using the traditional "direct store" method implies that the solution is both temporally and spatially periodic (standing wave solution). In an actual machine, blades are never exactly identical due to manufacturing imperfections, which result in non-identical vibration frequencies and phase shifts (mistuning) of the blades in a blade row. There are also evidences that show certain intentional mistuning may improve the flutter characteristics of a blade row. For such cases, the flow is no longer periodic in either space or time. Therefore, the traditional method with phase-shifted boundary conditions cannot be used. Computation for such flows must be done over multiple passages. In a previous work by Ji and Liu [5] a multigrid time-accurate Navier-Stokes code with a two-equation k-ω turbulence model was developed to calculate quasi-three-dimensional unsteady flows around multiple oscillating turbine blades.

*Graduate Researcher
†Associate Professor

The code is made parallel by using MPI so that multiple passages can be calculated without the use of phase-shifted periodic boundary conditions for blade flutter problems. The code runs efficiently on regular parallel computers or networked clusters of workstations or PCs. Communication is kept minimum since each blade passage is computed by one CPU and communication is only needed between this passage and its two immediate neighbors.

The standard configuration 4 of a turbine cascade by Bölcs and Fransson [1] is used as a test case. Damping coefficients are obtained for various inter-blade phase angles for the tuned case and compared with results for both phase-shift mistuning and frequency-mistuning. A method to calculate the damping coefficient for mistuned blades is presented. It is found that for this case, mistuning of phase-shift has small effects on the flutter characteristics, whereas mistuning of frequency has significant effect on the damping coefficients of each blade in the row. The overall effect of frequency-mistuning is to reduce the possibility of flutter. Especially alternate mistuning, where even and odd numbered blades oscillate with different frequencies, was found to have a strong stabilizing effect in various test configurations, e.g. Imregun and Ewins [3], Kaza and Kielb [6], Nowinski and Panovsky [8].

2 Computational Method

For a two-dimensional control Volume V with moving boundary ∂V the quasi-three-dimensional Favre-averaged Navier-Stokes equations with a k-ω turbulence model can be written as follows:

$$\frac{\partial}{\partial t}\iint_V \theta(x)\ \mathbf{w}\ dV + \oint_{\partial V} \theta(x)\ \mathbf{f}\ dS_x + \theta(x)\ \mathbf{g}\ dS_y = \oint_{\partial V} \theta(x)\ \mathbf{f}_\mu\ dS_x + \theta(x)\ \mathbf{g}_\mu\ dS_y + \iint_V \mathbf{S}\ dV \qquad (1)$$

where the vector $\mathbf{w}$ contains the conservative flow variables plus the turbulent kinetic energy k and the specific dissipation rate ω, in the k-ω turbulence model by Wilcox [9]. The vectors $\mathbf{f}, \mathbf{f}_\mu, \mathbf{g}, \mathbf{g}_\mu$ are the Euler fluxes and viscous fluxes in the x- and y-directions, respectively. $\theta(x)$ is introduced to account for variations in the streamtube thickness, and the source vector $\mathbf{S}$ includes terms due to the variation of $\theta(x)$. A detailed description of these terms can be found in [5].

A finite-volume method is used for spatial discretization. Equation (1) can then be written in semidiscrete form:

$$\frac{d\mathbf{w}}{dt} + \mathbf{R}(\mathbf{w}) = 0 \qquad (2)$$

where $\mathbf{R}$ is the vector of residuals, consisting of the spatially discretized flux balance of Equation (1). Time accuracy is achieved by using a second order implicit time-discretization scheme which is recast into a pseudo-time formulation, as proposed by Jameson [4]:

$$\frac{d\mathbf{w}}{dt^*} + \mathbf{R}^*(\mathbf{w}) = 0 \qquad (3)$$

For each physical time step in Equation (2) the solution is sought by solving Equation (3) for a steady-state in pseudo-time t^*. The benefit of this reformulation is that convergence acceleration techniques such as local time stepping, residual smoothing and a multigrid method can be used in pseudo-time without sacrificing time accuracy. At the boundaries between the passages a periodic boundary condition has to be applied:

$$\mathbf{w}_l = \mathbf{w}_u(x, t - \sigma/\omega) \qquad (4)$$

where subscripts l and u denote the lower and upper boundaries of a blade passage in Figure (1), σ is the IBPA, and ω is the angular frequency of the blade vibration. In order to perform calculations with

mistuned blades, the conventional direct store method by Erdos and Alzner [2], used to apply the phase-shifted periodic boundary condition, is replaced by pure periodic boundary conditions through the use of multiple passages as shown in Figure (1). Although this limits the inter-blade phase angle to be discrete numbers, it has the advantage of extending the calculations to a full annulus with nonperiodic motions and mistuned blades. The IBPA σ and the oscillation frequency ω can vary from blade to blade, which allows the investigation of both phase-mistuning and frequency-mistuning.

Figure (2) shows a cylindrical cut of a blade passage. The x coordinate is along the engine axis. The y coordinate is the circumferential coordinate, which is equivalent to $r\theta$ for a cylindrical cut at radius r, c is the chord length of the blade profile and c_x is the axial chord. The blades are assumed to be rigid and follow a motion of a combined bending and torsion mode. For the m-th blade, the bending and torsion motions can be specified as

$$\vec{h}^{(m)}(t) = a\left(\mu_x \vec{e}_x + \mu_y \vec{e}_y\right) e^{i(\omega_m t + \varphi_m)} \tag{5}$$

$$\alpha^{(m)}(t) = a(\mu_\alpha / c) e^{i(\omega_m t + \varphi_m)} \tag{6}$$

where α is positive anti-clockwise in Figure (2). If $\vec{h}(t)$ is written as

$$\vec{h}^{(m)}(t) = h_x^{(m)}(t)\vec{e}_x + h_y^{(m)}(t)\vec{e}_y \tag{7}$$

we can write

$$\begin{bmatrix} h_x^{(m)}(t) \\ h_y^{(m)}(t) \\ \alpha^{(m)}(t) \end{bmatrix} = a \begin{bmatrix} \mu_x \\ \mu_y \\ \mu_\alpha / c \end{bmatrix} e^{i(\omega_m t + \varphi_m)} \quad , \qquad m = 0, 1, 2, ... \tag{8}$$

where m stands for the blade number; $\omega_m = 2\pi f_m$ and φ_m are the angular frequency and the phase of the forced vibration of blade m. In the tuned case, the constant inter-blade phase angle is $\sigma = \varphi_m - \varphi_{m-1}$. The parameter

$$\mu = \begin{bmatrix} \mu_x \\ \mu_y \\ \mu_\alpha \end{bmatrix} \tag{9}$$

characterizes the specified modal shape of the combined bending and torsion motion; a is a general dimensionless amplitude. The modal parameters μ_x, μ_y, and μ_α all have the dimension of length. In general, they may be complex numbers when there are phase differences among the x, y bending motions and the torsion motion. However, standard configuration 4 does not include torsional vibration, so that the current work is performed with a pure bending mode, with a bending angle

$$\delta = \tan^{-1}(\mu_y / \mu_x)$$

A parallel algorithm is implemented in which each processor computes the flow through one blade passage, and communication between blade passages is achieved by using MPI. The method scales very well on both parallel computers and networked workstations. The accuracy of the numerical method and the efficiency of the parallel implementation have been validated in [5].

3 Results and Discussions

3.1 Computation for Tuned Blades

The case 552B of standard configuration 4 with inlet Mach number $M_1 = 0.28$, outlet isentropic Mach number $M_{is,2} = 0.90$ and inlet flow angle $\beta_1 = -45^\circ$ is chosen for comparison. Earlier comparisons

between Euler and Navier-Stokes results in [5] did not indicate significant viscous effects with this configuration. Therefore, in the current work only Euler calculations are performed. Figure (3) shows the steady-state isentropic Mach number distribution over the blade surface. The numerical results agree very well with the experimental data.

The first harmonic amplitude and phase angle of the unsteady pressure coefficient are plotted in Figures (4) and (5). The trends of computational and experimental data match reasonably well. However, there are discrepancies in both the amplitude and phase. The calculation predicts much higher amplitudes over the front half-chord, a phenomenon which was already mentioned in [1]. This is in particular true for inter-blade phase angles around 90°. The resulting differences in the damping coefficient around 90° are of similar order (Figure (6)), whereas in the region of instability much better agreement is achieved. For the investigation of mistuning effects, another test case with $\beta_1 = -10°$ was chosen, because it is unstable over a slightly larger IBPA-range (Figure (6)).

3.2 Validation of the Method of Influence Coefficients

Although the method presented in this paper provides a powerful tool for calculating the complete unsteady flow field with multiple oscillating blades, it is desirable, particularly in experiments, to only need to oscillate one blade. This can be expected to be possible when the flow exhibits no strongly nonlinear phenomena like oscillating shocks or separation regions. If this is the case, the superposition principle should hold: given the influence of one blade on its neighbors, the solution on each blade can be obtained by superimposing the contributions of all neighbors. The method of influence coefficients simplifies both experiment and computation to a large extend and has been used and validated for several test cases, e.g. [7], [8]. The contributions of a vibrating blade on its stationary neighbors are expressed in terms of magnitude and phase of blade oscillation and influence coefficients. The coefficient magnitude and phase are different for each neighbor blade. A summation over all blades yields an approximate solution. The accuracy certainly depends on the actual linearity of the flow. As a secondary objective of this paper we demonstrate in this subsection the validity of this superposition principle by using our multipassage code. In the current work the superposition is done in the time domain, without decomposing the influence into blade oscillation and coefficient. A single run is performed, with a total number of N blades, only one of which, say blade number 0, is vibrating. The time dependent distributions of the pressure coefficient describe the influence of the vibrating blade on its neighbors. For the complete solution with all blades oscillating at the same frequency and amplitude, the pressure coefficients are simply added, applying the desired phase shifts.

$$C_{p,i}(x,t) = \sum_{j=0}^{N-1} C_{p,(N+i-j)mod\ N,\,0}(x, t + \varphi_j - \varphi_0) - (N-1) \cdot \overline{C_p}(x) \tag{10}$$

where $C_{p,i}$ is the pressure coefficient on blade i, $C_{p,k,0}$ is the contribution to the pressure coefficient on blade k, caused by oscillation of blade 0, φ_k is the oscillation phase of blade k, $\overline{C_p}$ is the steady-state pressure coefficient, and N is the total number of blades.

Only one Euler calculation is needed to obtain results for a number of inter-blade phase angles, depending on the number of blades in the calculation. As an example, Figure (7) shows the time dependent pitchwise force coefficient, from the complete Euler solution and from superimposed single blade contributions, respectively, for $IBPA = 90°$. The different methods agree very well, strongly indicating linear flow behavior. Figure (8) compares the results for the damping coefficients, and confirms linearity for all inter-blade phase angles. Note that the largest discrepancies appear at inter-blade phase angles close to 90°. In that sense, Figure (7) shows the worst case.

3.3 Phase-Mistuning

In this and the next subsections we proceed to perform studies on mistuned blade rows by performing complete unsteady calculations with multiple oscillating blades.

In the tuned case all blades oscillate with a same frequency ω and with the same phase difference σ between each pair of adjacent blades as defined by Equation (8). A simple way of mistuning the system is to slightly change the phase of one of the blades, so that the IBPA is not constant over the blade row. For example, Blade 1 in Figure (1) can be mistuned by a phase shift $\Delta\sigma$, so that

$$\begin{bmatrix} h_x^{(1)}(t) \\ h_y^{(1)}(t) \\ \alpha^{(1)}(t) \end{bmatrix} = a \begin{bmatrix} \mu_x \\ \mu_y \\ \mu_\alpha/c \end{bmatrix} e^{i(\omega t+\sigma+\Delta\sigma)} \tag{11}$$

The phase difference between blade 0 and blade 1 then becomes $\sigma+\Delta\sigma$, and $\sigma-\Delta\sigma$ between blade 1 and blade 2, whereas all other IBPAs remain at the original value σ.

For the case of 4 passages shown in Figure (1) and $\Delta\sigma = +10°$, Figure (9) and 10 show the damping coefficient Ξ as a function of σ, which is now the *average* IBPA. Using only four passages limits the choice for σ to $0°, 90°, 180°$ and $270°$. For these inter-blade phase angles the results for the tuned case, already shown in Figure (6), are also plotted.

It is obvious that, due to mistuning, the damping coefficient Ξ varies for different blades. However, only blade 0 and blade 1 show significant changes with respect to the tuned case. The blade order is such that blade number i+1 is adjacent to the suction side of blade number i. Therefore it is the suction sides of blade 0 and blade 1 that are directly affected by mistuning blade 1. Although blade 2 is adjacent to the mistuned blade it is not affected very much. The mistuned blade concerns blade 2 mainly on the less sensitive pressure side.

The changes in damping coefficient and therefore stability go in opposite directions for blade 0 and blade 1. Blade 0 mainly feels a phase difference of $\sigma + 10°$ at its suction side. At any σ the mistuned value of Ξ qualitatively changes towards the tuned damping coefficient for $\sigma + 10°$. The stability of blade 1, being dominated by a phase difference $\sigma - 10°$, behaves in a similar way. These explanations for the qualitative influence of this kind of mistuning also hold for a negative $\Delta\sigma = -10°$ (Figures (11) and (12)). It can be seen that $\Delta\Xi$ is small at relative extrema and large in between. In general, both absolute value and sign of $\Delta\Xi$ appear to depend on the imposed mistuning phase difference $\Delta\sigma$ and the slope of the tuned stability curve, if $\Delta\sigma$ is considerably small:

$$\Delta\Xi \sim \left.\frac{\partial\Xi}{\partial\sigma}\right|_{tuned} \cdot \Delta\sigma$$

3.4 Frequency-Mistuning

Another way to introduce mistuning is to let the blades oscillate with slightly different frequencies. In a first study this is done again with a single blade out of four, i.e. blade 1 in Figure (1) vibrates with a slightly higher frequency than the other blades.

$$\begin{bmatrix} h_x^{(1)}(t) \\ h_y^{(1)}(t) \\ \alpha^{(1)}(t) \end{bmatrix} = a \begin{bmatrix} \mu_x \\ \mu_y \\ \mu_\alpha/c \end{bmatrix} e^{i(\omega t+\Delta\omega t+\sigma)} \tag{12}$$

For $\Delta\omega = \frac{1}{14}\omega$ the influence on the damping coefficient is shown in Figures (13) and (14). The damping of the mistuned blade 1 is independent from the inter-blade phase angle. This is not

surprising because the concept of a constant IBPA does not apply on blade 1. The phase differences with respect to the three other blades, respectively, are continuously changing in time. After one period of the mistuned system, blade 1 has gone through all IBPAs from 0° to 360°. Its damping coefficient is close to the tuned Ξ averaged over the IBPA, which is a positive (stable) value. Blade 0 still has constant IBPAs in respect to blade 2 and 3. The permanently changing phase difference with respect to its suction side neighbor (blade 1), however, also weakens the IBPA dependence of blade 0. It becomes stable at any IBPA. Blade 2 and 3 hardly change compared to the tuned case.

The positive effect on the mistuned blade itself and on one of its neighbors leads to the idea of alternate mistuning: every second blade in the row is mistuned in the same way,

$$\begin{bmatrix} h_x^{(m)}(t) \\ h_y^{(m)}(t) \\ \alpha^{(m)}(t) \end{bmatrix} = a \begin{bmatrix} \mu_x \\ \mu_y \\ \mu_\alpha / c \end{bmatrix} e^{i(\omega t + \Delta\omega t + m\sigma)} \quad , \qquad m = 1, 3, 5, ... \tag{13}$$

Figure (15) shows the result for the same frequency difference as in the previous case, but here imposed on both blade 1 and blade 3. In this case, all blades are stable with little dependence on the IBPA. This phenomenon has also been described for other test cases and vibration modes, see e.g. the experimental results in [8]. A dependence on the IBPA can only be introduced by the second neighbors, because only these oscillate with the same frequency. We already know from the previous subsection that the influence by second neighbors is much smaller than by the direct suction side neighbor, therefore there is not much variation with the inter-blade phase angle. The diagram also shows that alternate mistuning changes the period of the damping coefficient from 360° to 180°. This again means that it is not meaningful to talk about an IBPA between adjacent blades in such cases. The only IBPA to be considered is the one between every two blades. The effect of alternate mistuning in this case can be thought of as splitting the blade row into two staggered tuned systems damping each other. The damping coefficient depends on the oscillation frequency. The blade oscillating at the higher frequency appears to be more stable. The effect of frequency-mistuning should not be thought of as an introduction of new damping. It is rather taking away the IBPA specific influence of neighboring blades. Whether this leads to more or less stability than in the tuned case depends on the phase averaged damping coefficient at the given frequency, and on the actual phase angle of the tuned case. It may be expected, that this type of mistuning might introduce absolute instability if the tuned blades exhibit instability over a majority of the IBPA range. We have yet to find such a test case and verify this conjecture.

4 Conclusions

A computational method for predicting flutter of turbomachinery cascades with mistuned blades is presented. The method is based on solving the unsteady Euler/Navier-Stokes equations through multiple blade passages on a parallel computer. Each individual blade is capable of moving with its own independent frequency and also phase angle, therefore allowing flutter predictions with either frequency or phase-mistuning. Computations for a turbine blade row show that mistuning in phase has relatively small effect on the flutter characteristics of the blade row. On the other hand, frequency-mistuning can have significant influence on the damping coefficient of the mistuned blade and its adjacent neighbor. The result is a damping coefficient averaged over the complete IBPA range (0° - 360°) since the actual phase differences between the mistuned blade and its adjacent blades are constantly changing within that range due to the frequency difference. If the blade is stable over most of the IBPA range in the tuned case, the blade will then become stable in a overall sense in the mistuned case. When this effect is made use of in constructing a blade row with alternating mistuned

blades, it is found that frequency-mistuning may stabilize all blades over the whole effective IBPA range. However, it should be mentioned that this effect may not show as clearly if the flow behaves in a nonlinear way. In that case the influence of second neighbors may be much more significant than in the investigated test case. Furthermore, in a real configuration mechanical coupling between blades may decrease the effect or even the applicability of alternate frequency-mistuning.

The presented computational method is also used to verify the method of influence coefficients for a case with very little nonlinear effects.

Acknowlegdements

The authors would like to thank Dr. Stefan Irmisch and Dr. Thomas Sommer at ABB Power Generation Limited in Baden, Switzerland, for useful discussions on the topic of mistuning. Computations have been performed on the Aeneas parallel computer and the HP Exemplar SPP2000 parallel computer, both at UC Irvine.

References

[1] Bölcs, A., and Fransson, T. H., "Aeroelasticity in Turbomachines - Comparison of Theoretical and Experimental Cascade Results", Communication du Laboratoire de Thermique Appliquée et de Turbomachines, No. 13, Ecole Polytechnique Fédérale de Lausanne (EPFL), Lausanne, 1986.

[2] Erdos, J. I., and Alzner, E., "Numerical Solution of Periodic Transsonic Flow Through a Fan Stage", NASA CR-2900, 1978

[3] Imregun, M., and Ewins, D. J., "Aeroelastic Vibration Analysis of Tuned and Mistuned Blade Systems", Unsteady Aerodynamics of Turbomachines and Propellers, Symposium Proceedings, Cambridge, England, Sept. 1984.

[4] Jameson, A., "Time Dependent Calculations Using Multigrid, with Applications to Unsteady Flows Past Airfoils and Wings", AIAA Paper 91-1596, June 1991

[5] Ji, S. and Liu, F., "Flutter Computation of Turbomachinery Cascades Using a Parallel Unsteady Navier-Stokes Code", AIAA Journal, Vol. 37, No. 3, March 1999

[6] Kaza, K. R. V., and Kielb, R. E., "Flutter and Response of a Mistuned Cascade in Incompressible Flow", AIAA Journal, Vol. 20, No. 8, pp. 1120-1127, Aug. 1982

[7] Körbächer, H., and Bölcs, A., "Experimental Investigation of the Unsteady Behaviour of a Compressor Cascade in an Annular Ring Channel", Paper presented at the 7^{th} International Symposium on Unsteady Aerodynamics and Aeroelasticity of Turbomachinery, Fukuoka, Japan, Sept. 25-29., 1994

[8] Nowinski, M., and Panovsky, J., "Flutter Mechanisms in Low Pressure Turbine Blades", ASME Paper 98-GT-573, 1998

[9] Wilcox, D. C.,"Reassessment of the Scale-Determining Equation for Advanced Turbulence Models", AIAA Journal, Vol. 26, No. 11, pp. 1299-1310, 1988

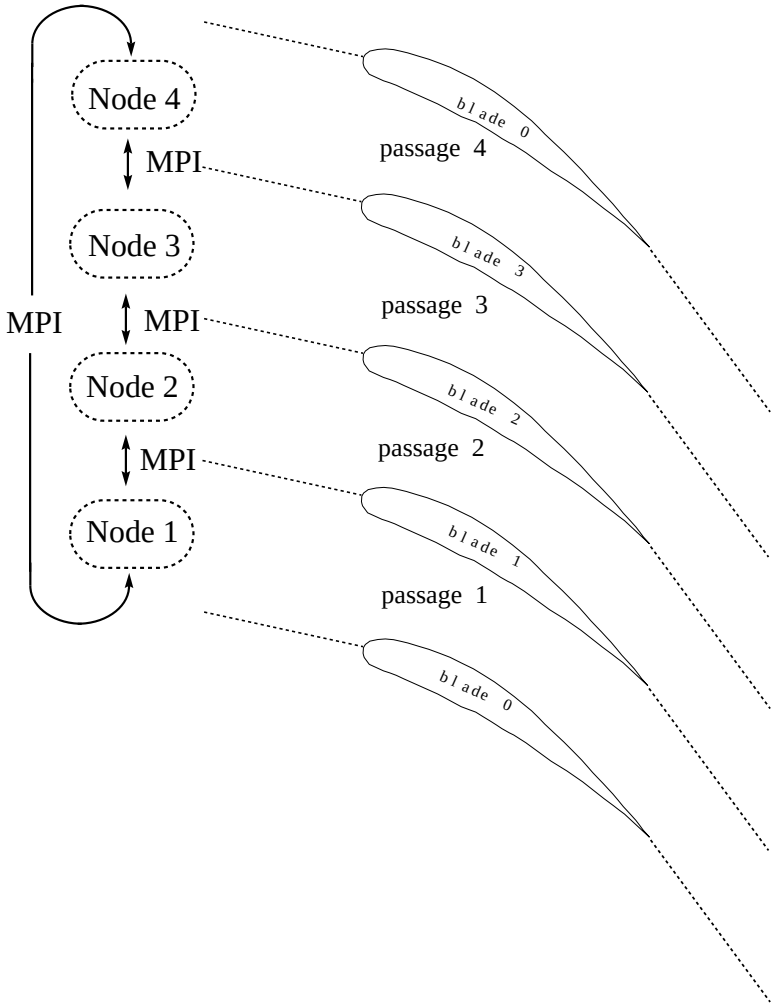

Figure 1: Multiple passage computation using MPI

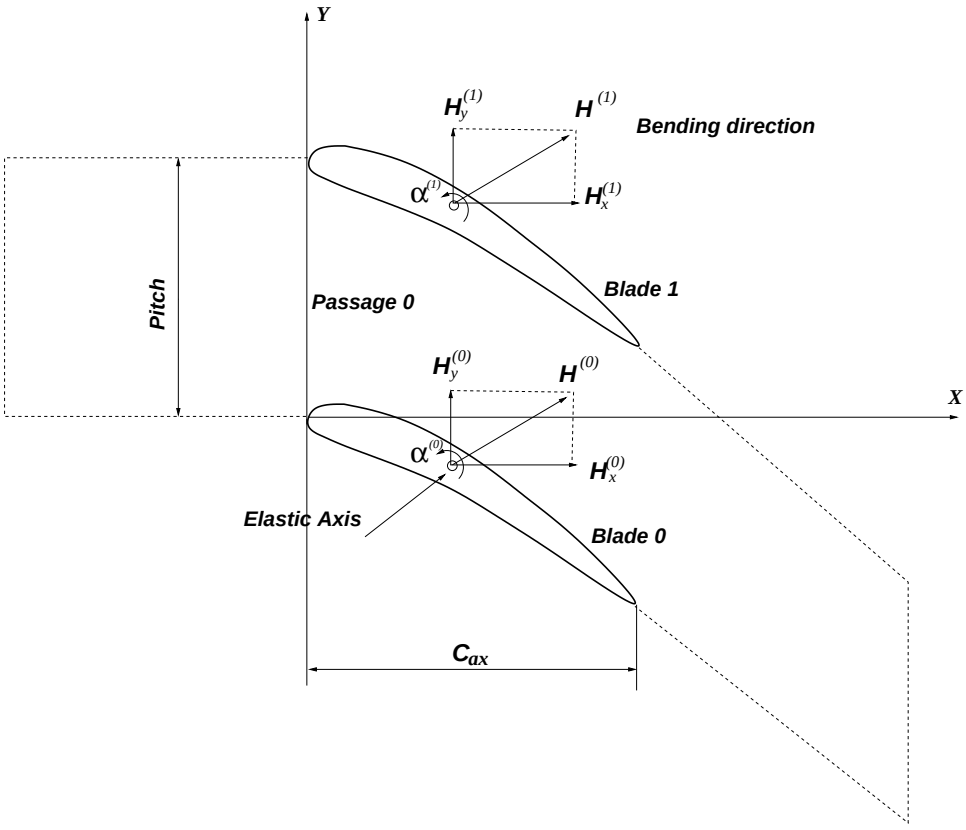

Figure 2: Blade geometry and motion definition

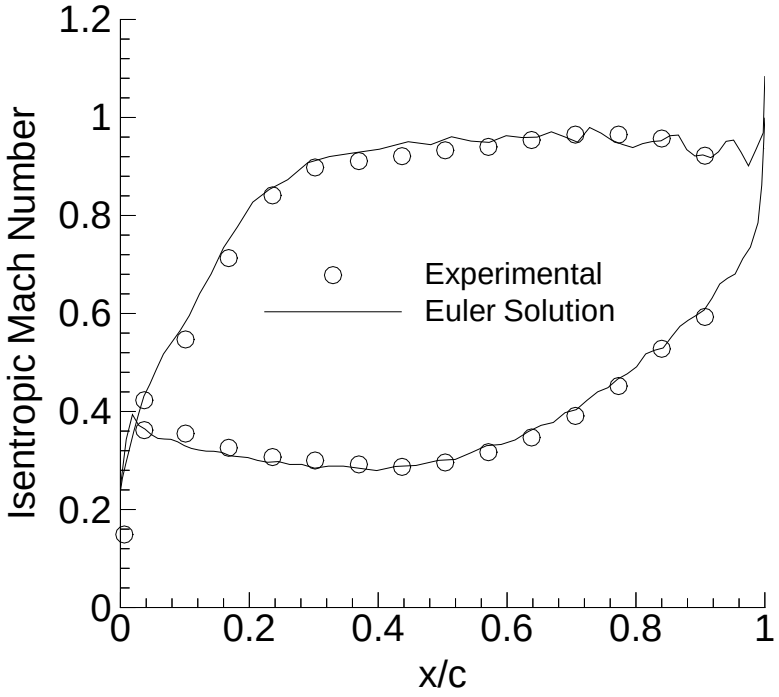

Figure 3: Steady-state isentropic Mach number distribution over the blade

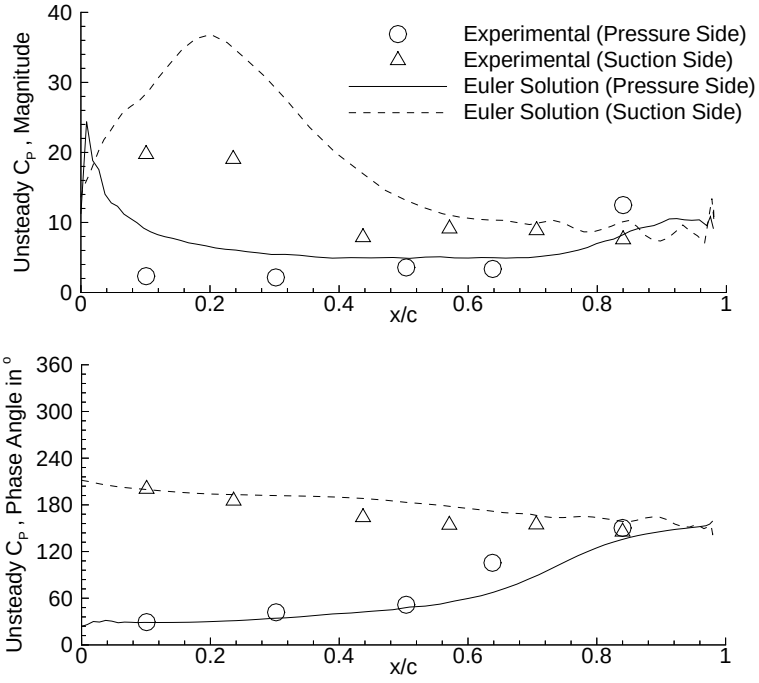

Figure 4: Amplitude and phase of the first harmonic unsteady pressure coefficient over the blade with $IBPA = 180^{\circ}$

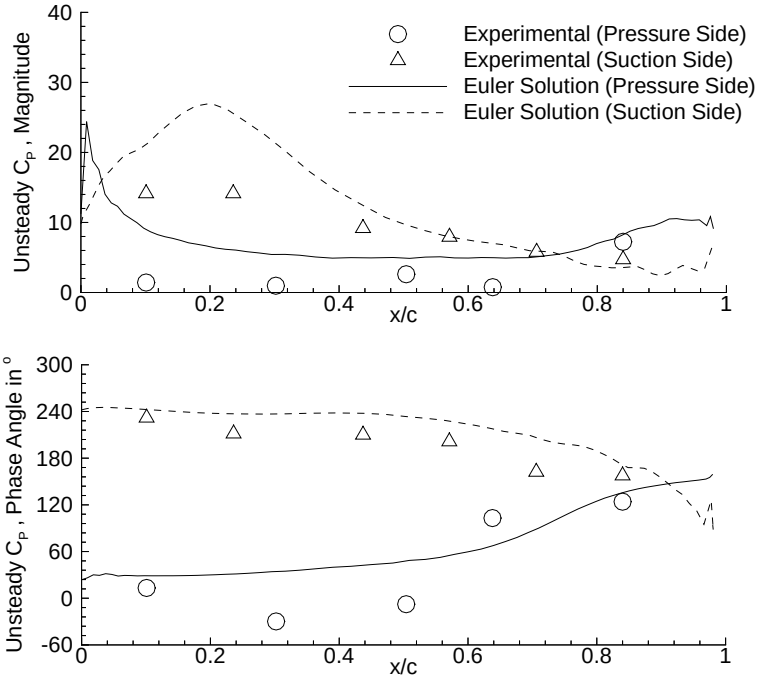

Figure 5: Amplitude and phase of the first harmonic unsteady pressure coefficient over the blade with $IBPA = 90°$

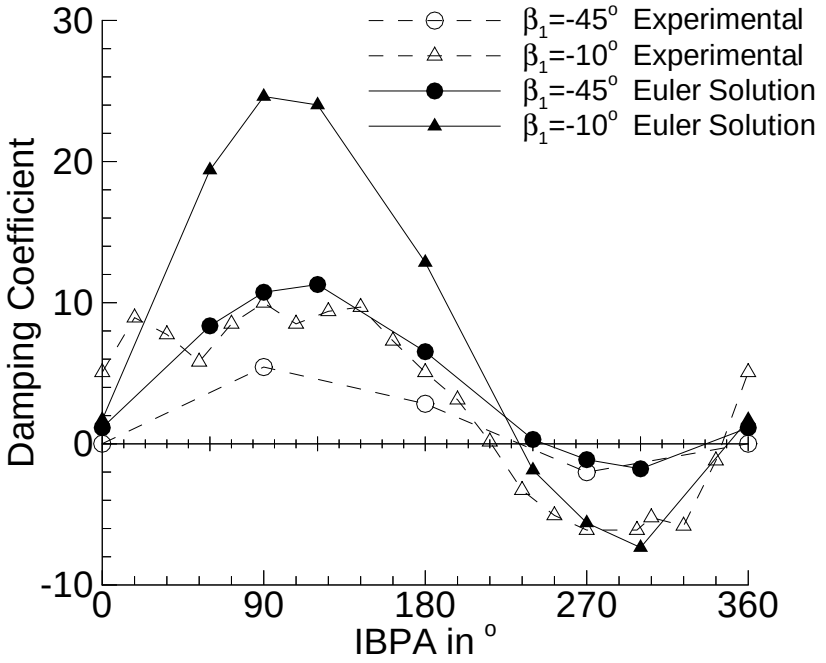

Figure 6: Damping coefficient over IBPA with $\beta_1 = -45°$ and $\beta_1 = -10°$

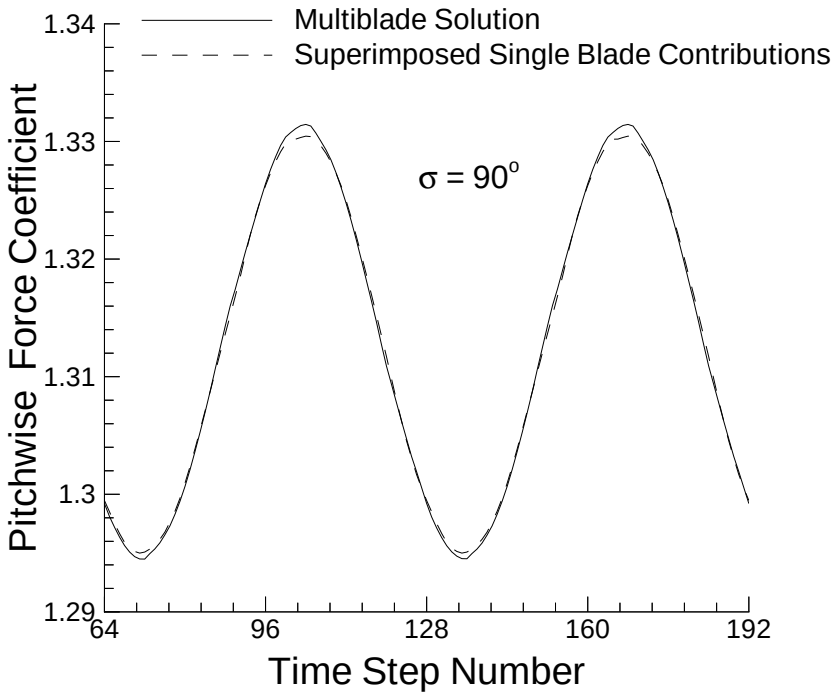

Figure 7: Pitchwise force coefficient - multiblade calculation vs. superposition method

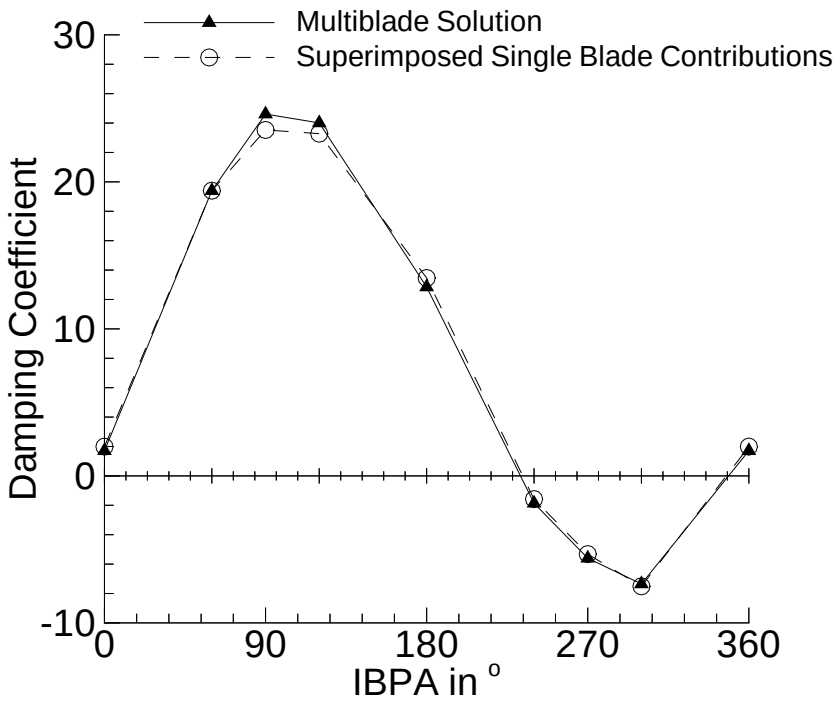

Figure 8: Damping coefficient - multiblade calculations vs. superposition method

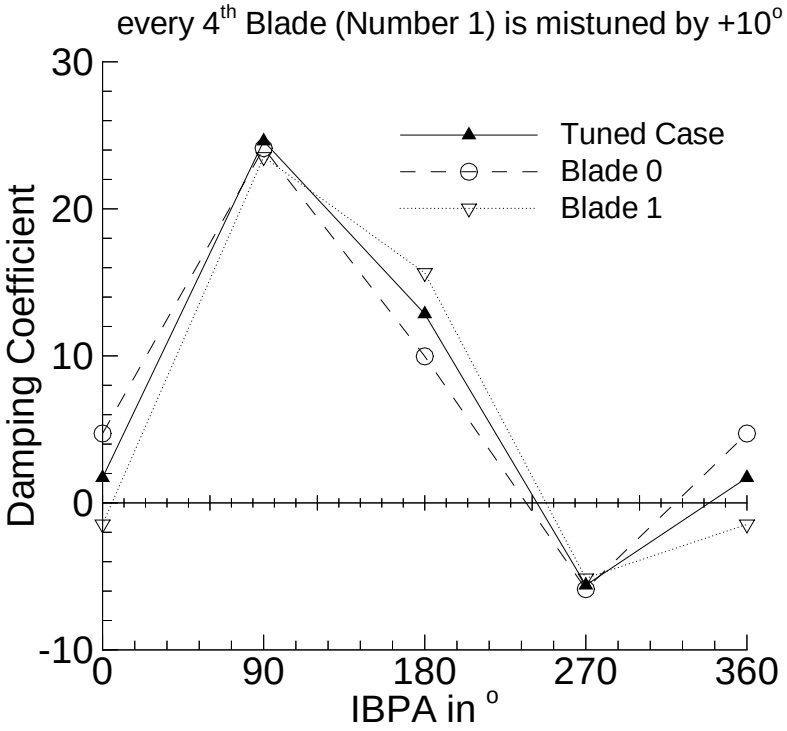

Figure 9: Damping coefficient vs. IBPA for blade 0 and 1. Blade 1 is mistuned in phase by $+10°$.

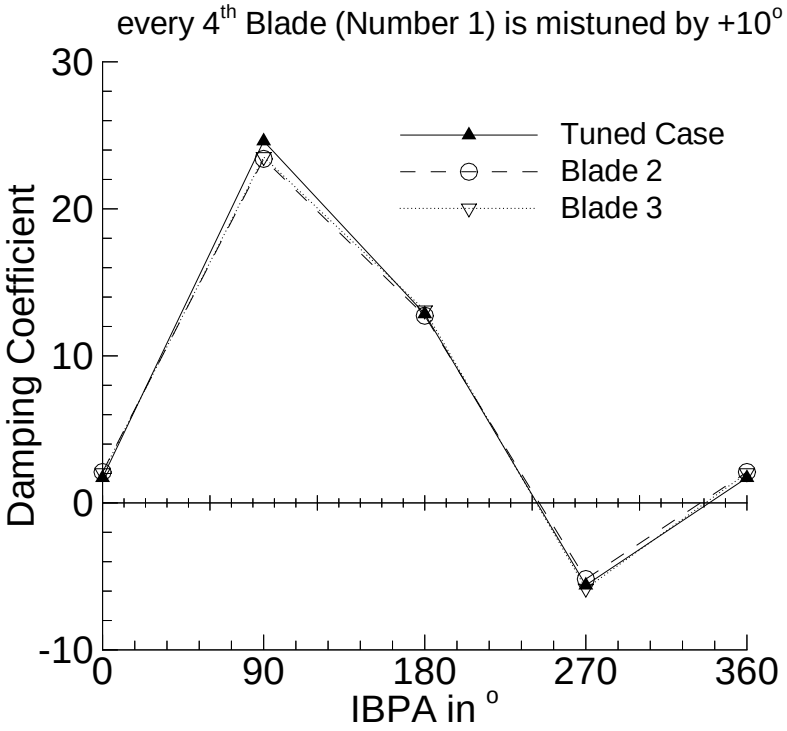

Figure 10: Damping coefficient vs. IBPA for blade 2 and 3. Blade 1 is mistuned in phase by +10°.

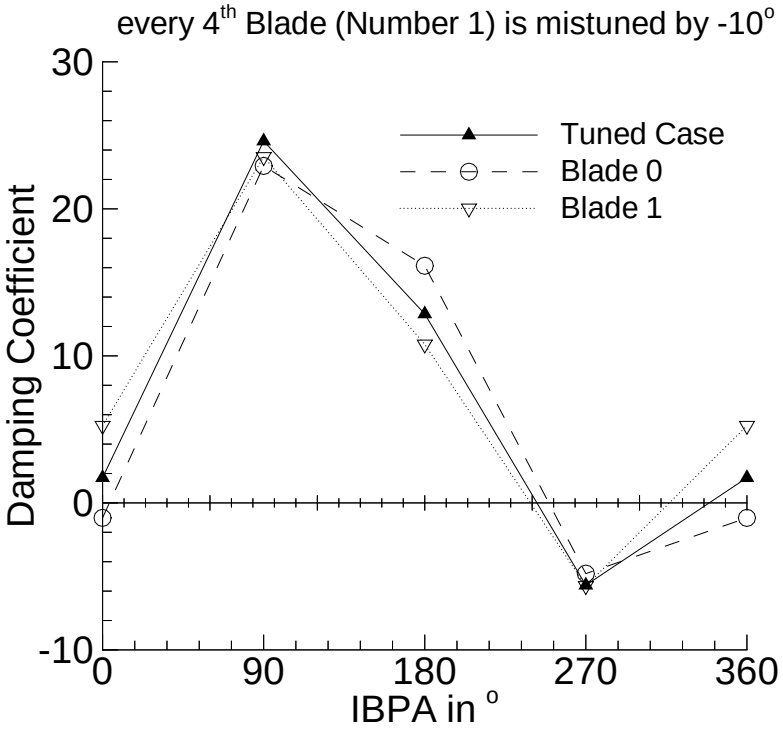

Figure 11: Damping coefficient vs. IBPA for blade 0 and 1. Blade 1 is mistuned in phase by $-10°$.

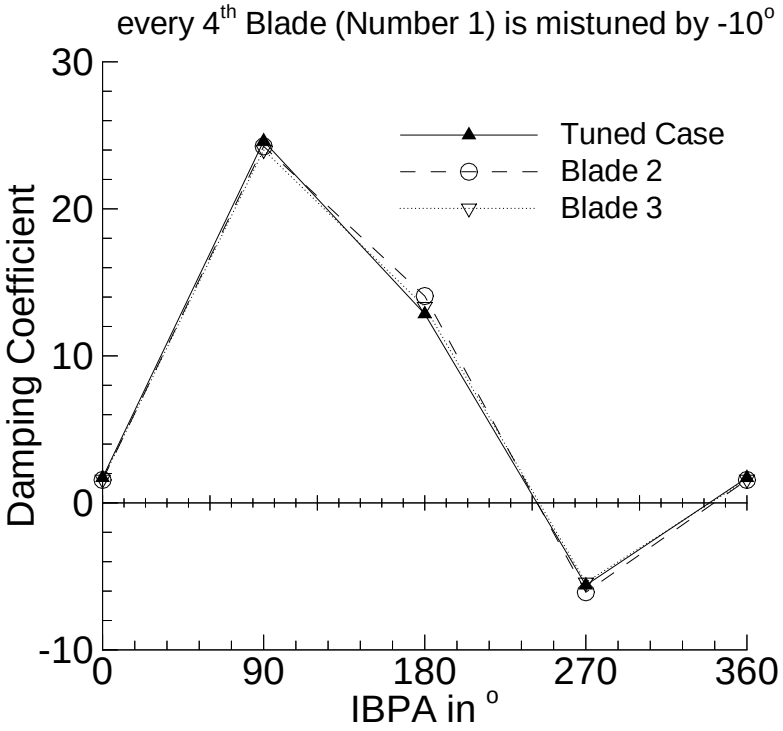

Figure 12: Damping coefficient vs. IBPA for blade 2 and 3. Blade 1 is mistuned in phase by $-10°$.

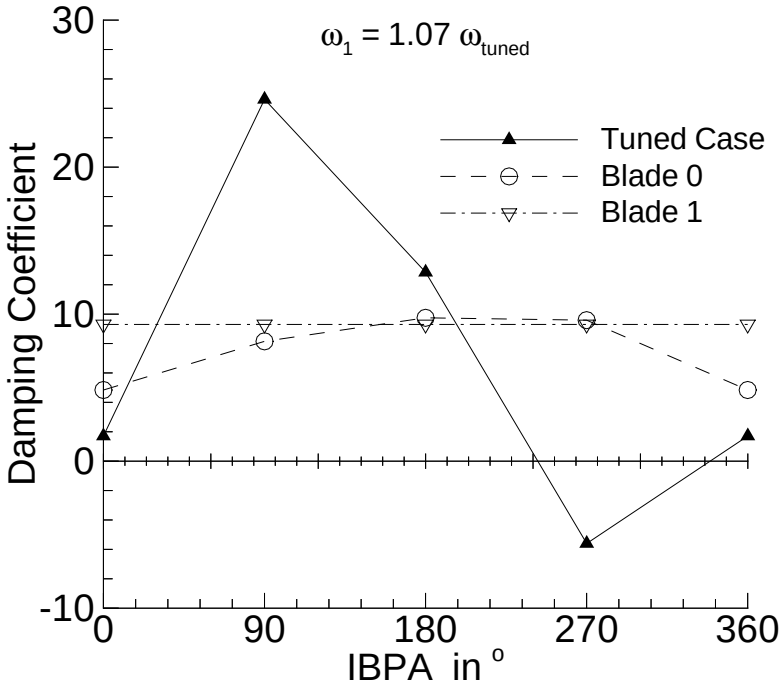

Figure 13: Damping coefficient vs. IBPA for blade 0 and 1. Blade 1 is mistuned in frequency by +7%.

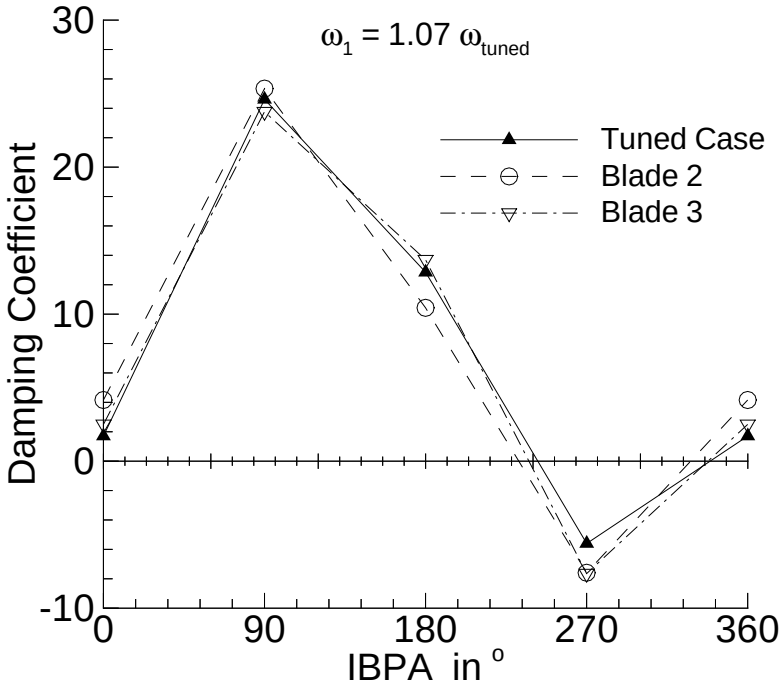

Figure 14: Damping coefficient vs. IBPA for blade 2 and 3. Blade 1 is mistuned in frequency by +7%.

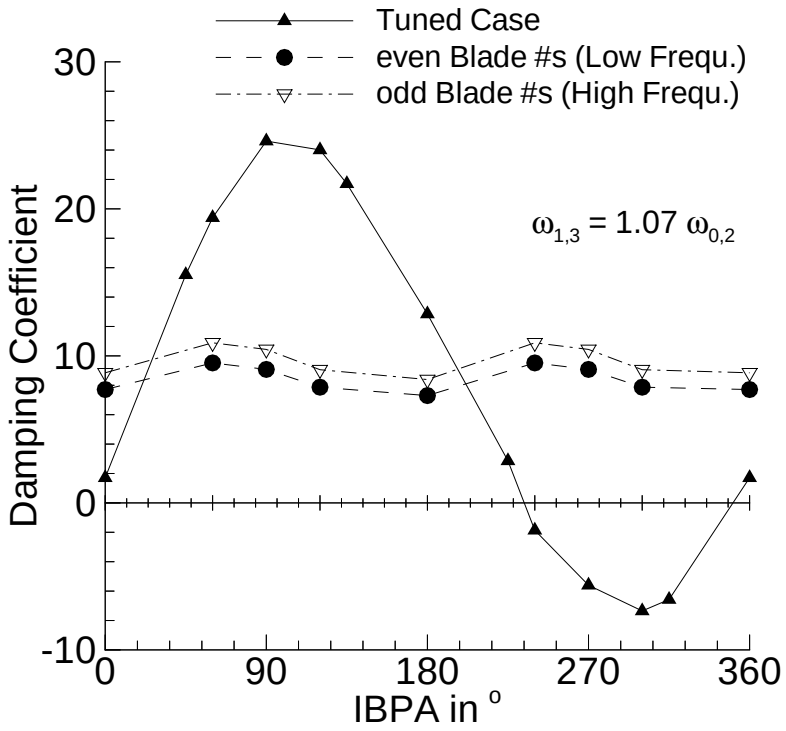

Figure 15: Damping coefficient vs. IBPA. Odd numbered blades are mistuned in frequency by +7%.